Study of The Effect of Draw-bead Geometry on Stretch Flange Formability

O.S. Orlov*, S. L. Winkler*, M. J. Worswick*, D.J. Lloyd**, M.J. Finn**

*Department of Mechanical Engineering. University of Waterloo, Waterloo, N2L 3G1, CANADA
**ALCAN International Ltd., Kingston R&D Centre PO Box 8400, Kingston, Ontario, K1S 5L9, CANADA

Abstract. A fully instrumented stretch flange press equipped with a back-up punch and draw-beads near the specimen cutout area is simulated. The utilization of different draw-bead geometries is examined numerically to determine the restraining forces, strains and amount of damage generated in stretch flanges during forming. Simulations of the forming process are conducted for 1mm AA5182 sheets with circular cutouts. The damage evolution with the deformed specimens is investigated using the explicit dynamic finite element code, LS-DYNA, with a modified Gurson-based material model. It was found that double draw-beads can provide the same amount of restraining force as single draw-beads, but at reduced levels of damage.

INTRODUCTION

Stretch flanges or Z-flanges are common features in automotive sheet metal stampings, such as structural inner panels that contain window or door cutouts. In stretch flange forming operations [1,2], draw-beads are widely employed to control material feed and thinning by providing additional restraining force as the sheet metal flows through them. These restraining forces act locally and allow the use of lower overall clamping forces during forming. The amount of restraint and damage induced in a material are characteristic of draw-beads used and are highly dependent on draw-beads' geometry.

Draw-beads have been extensively studied over the last few decades by various researchers and a large number of draw-bead designs have been proposed. Many researchers [3-5] have worked on a class of active draw-beads that are capable of variable penetration depth and restraining forces. Others, such as Kaum *et al.* [6], have carried out studies on multiple draw-bead designs that consist of single draw-beads of different types. A recent review by Xu *et al.* [7] summarizes the various types of draw-bead designs studied, as well as their finite element modeling and restraining force predictions.

Commercial part forming operations are usually simulated using a finite element package prior to tooling fabrication. In general, the mesh utilized should be sufficiently fine in order to capture effects from small geometrical features. However, draw-beads are usually very small in size, and modeling material flow through them would result in additional computational expenses due to the high number of elements required. Therefore, draw-beads are modeled using "equivalent draw-beads" - regions that provide additional restraining force at specific locations of the sheet, to avoid redundant mesh refinement and reduce computational time. Different types of draw-beads can be tested to determine their restraining forces and then implemented as equivalent draw-beads during finite element analysis. A damage parameter is required to fully describe the draw-bead profile since the damage levels produced by different draw-beads varies with the draw-bead's curvature radii and the number of bends and unbends it contains. Hence, the objective of this research is to investigate the effect of draw-bead geometry on stretch flange formability by comparing the restraining forces and damage induced by a variety of single and double draw-beads using the explicit dynamic finite element code, LS-DYNA, with a modified Gurson-based material model.

CP712, *Materials Processing and Design: Modeling, Simulation and Applications,* NUMIFORM 2004,
edited by S. Ghosh, J. C. Castro, and J. K. Lee

PROCEDURE

Stretch-flange Forming Operation

Figure 1 shows a schematic view of a typical draw-bead application in a stretch-flange forming operation [8] from which it can be seen that the tooling geometry is axisymmetric. The draw-bead is employed to delay the cut-out expansion of the blank. Lock-beads are incorporated into the clamping system to prevent the sheet metal from feeding into the die cavity.

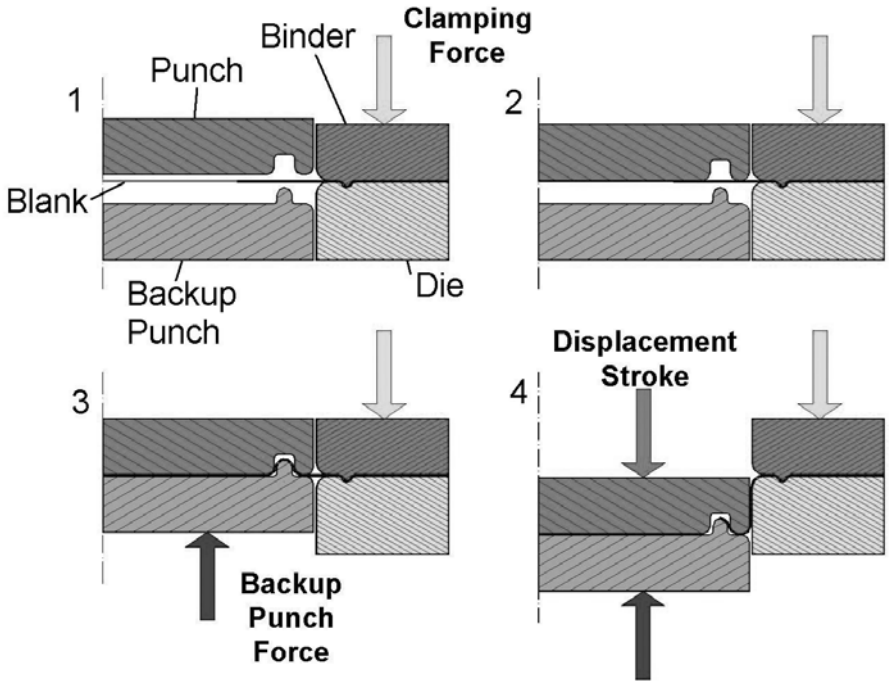

FIGURE 1. Schematic showing the sequence of events in a stretch-flange forming operation. 1) The blank is clamped. 2) The punch advances to the blank's surface. 3) The draw-bead closes. 4) A stretch flange is formed.

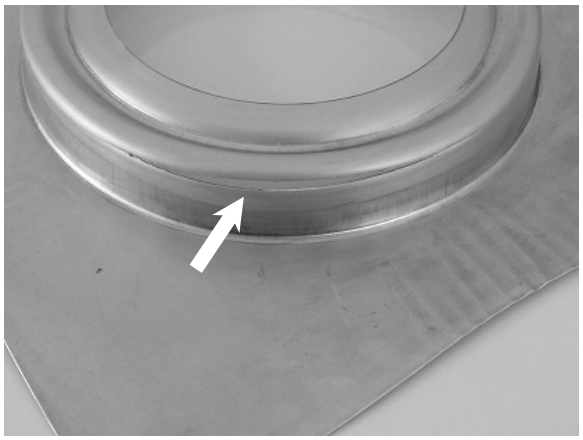

FIGURE 2. A stretch-flange with a circumferential crack.

A typical failure mode during such an operation is circumferential cracking along the flange wall as illustrated in Figure 2. The material in the cracked region has been repeatedly bent and unbent by flowing through the draw-bead profile and stretched in the circumferential direction. Draw-beads play a crucial role in stretch forming operations and improved draw-bead designs will allow for further optimization of this process.

Choice of the Draw-bead Profiles

Previous work done by Orlov *et al.* [9] suggests that similar levels of restraining forces but different levels of damage can be generated in a stretch flange by varying the geometry of the draw-bead used. The restraining forces imparted by draw-beads onto a material during forming are dependent on the draw-beads' curvature radii and the number of bends that the material has to flow through. Draw-beads with smaller curvature radii or multiple draw-beads with higher

number of bends exert more restraining force. In forming operations, draw-beads that are capable of providing sufficient restraint with minimal damage or loss of formability in the material are preferred.

The restraining forces and damage evolution generated by shallow single and double round draw-beads (Figure 3) with different radii are examined. Shallow draw-beads are selected for this investigation, since deeper draw-beads would only result in higher frictional forces due to the larger surface contact of the blank with the tooling.

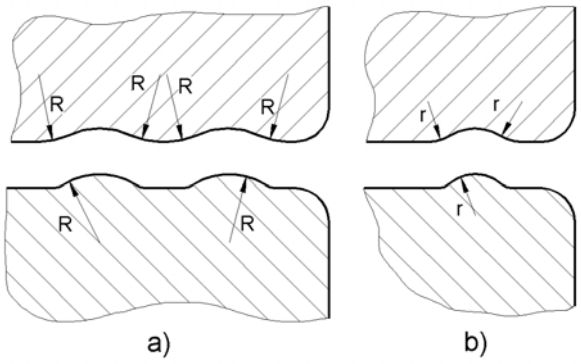

FIGURE 3. (a) Double draw-bead and (b) single draw-bead.

Numerical Investigation

Numerical simulations are conducted using the finite element package LS-DYNA [10], which utilizes a modified Gurson-based material model [11-13], to predict the damage evolution within the 1mm AA5182 sheet during stretch flange forming. Single and double round draw-beads profiles with curvature radii of 6, 8, 10, 12, 14 mm and 8, 10, 12, 14 mm, respectively, are investigated and compared.

The numerical investigation is divided into two stages:

- Stage I: Plane-strain simulation of a strip of 1mm AA5182 sheet pulled through the draw-bead is performed for each draw-bead geometry.
- Stage II: Selected draw-bead profiles are modeled in the axisymmetric simulations of a stretch flange forming operation.

Stage I is employed to estimate the restraining forces produced by the draw-beads, F_{DBEAD}, independent of the circumferential tension, $F_{CTENSION}$, that is present in stretch flanges. The total restraining force in stretch flange forming operations is given by:

$$F_{RSTRAIN} = F_{DBEAD} + F_{CTENSION}$$

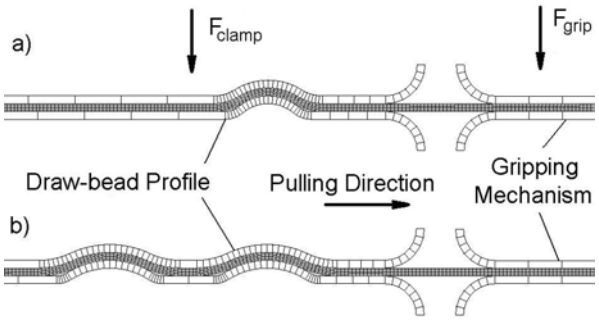

FIGURE 4. Geometry and finite element meshes of the single (a) and double (b) draw-bead profiles.

Plain strain strip results

Figure 4 shows the geometry and mesh used in the strip-pulling simulations for the 1mm AA5182 sheet. The strip is clamped between the male and female counterparts of the draw-beads on one side, and between two gripping plates on the other. Forces are applied to keep the draw-beads and the gripping plates closed, and restrain the material from slipping out of the gripping mechanism as it pulls the strip out of the draw-bead. The clamping force applied at the draw-beads is varied between 400 and 800 N/mm to study their effects on the material's damage evolution. Coefficient of friction values of 0.085 and 0.15 are used to simulate lubricated contact between the sheet and draw-bead, and dry contact between gripping plates and blank, respectively.

The maximum porosity values versus strain in the pulling direction and strain in the pulling direction versus restraining force, obtained from each simulation, are presented in Figures 5 and 6, respectively. Each data point on each curve corresponds to a different clamping force used in the simulations. Under plane-strain conditions, the strain in the pulling direction is proportional to the restraining force. The maximum porosity values and the restraining forces at 3% material strain for the various draw-beads are obtained by interpolating the results in Figures 5 and 6 are plotted against the curvature radii of the draw-beads in Figures 7 and 8. The value of 3% material strain is chosen as a representative value required in draw-beads within production tooling.

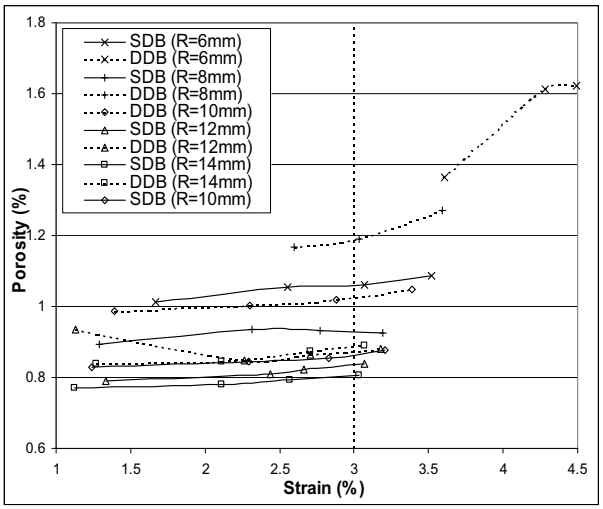

FIGURE 5. Maximum porosity versus strain in the pulling direction.

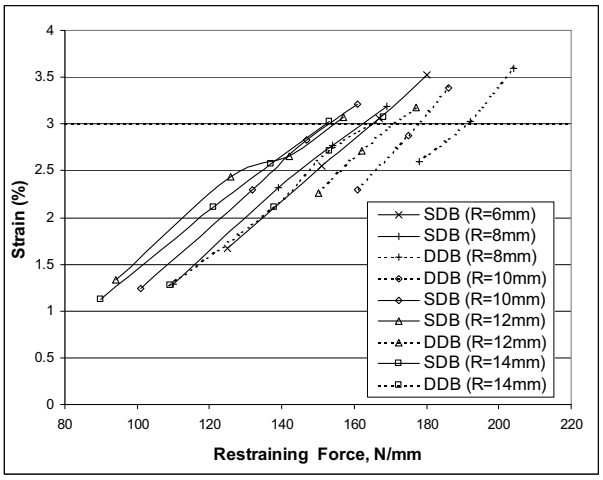

FIGURE 6. Strain in the pulling direction versus restraining force

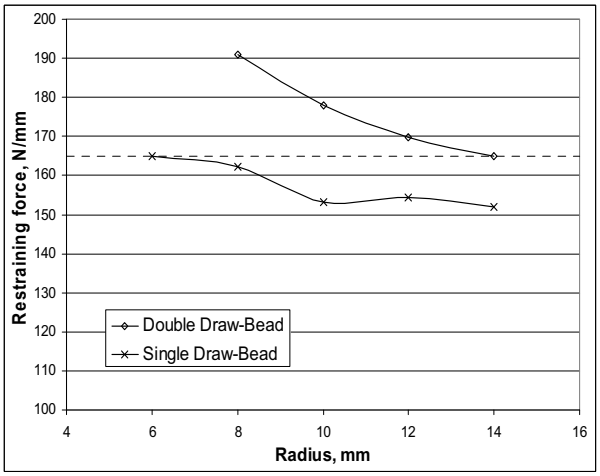

FIGURE 7. Draw-bead restraining force versus curvature radius at 3% material strain.

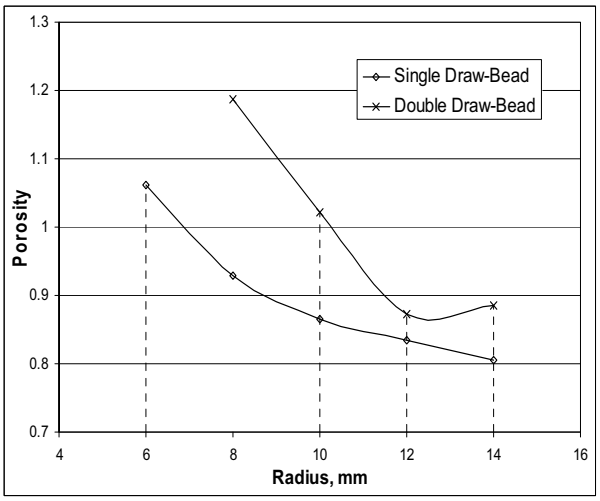

FIGURE 8. Maximum porosity versus curvature radius at 3% material strain.

Figure 7 shows that under plane strain conditions, similar restraining forces of roughly 165 N/mm are generated by single draw-beads of 6mm and double draw-bead of 14mm radius. Figure 8 shows that the double draw-beads with curvature radii of 10,12, and 14mm cause less damage in the metal strip than a single drawbead with a 6mm radius.

Axisymmetric stretch flange results

Based on the plane strain simulations, the 10, 12, and 14mm radii double draw-beads and the 6mm radius single draw-bead geometries were selected and utilized in axisymmetric stretch-flange forming simulations. The geometry and finite element meshes used in the axisymmetric simulations are illustrated in Figures 9 and 10.

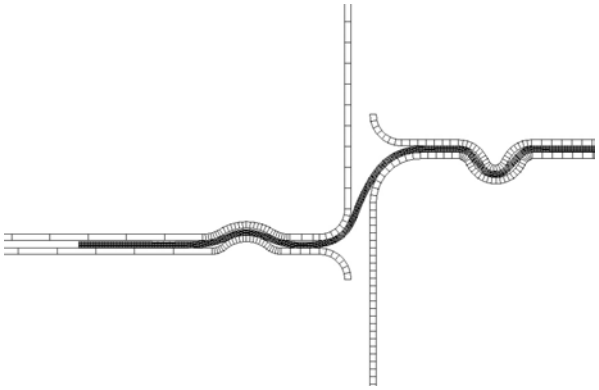

FIGURE 9. Geometry and finite element model of the stretch-flange forming operation with single draw-bead profile.

All simulations were conducted with the same backup punch force of 244.7 kN (55000 lbs) and a clamping force of 378.1 kN (85000 lbs). The total restraining force experienced by the blank can be calculated from the following equations:

$$F_{PUNCH} = F_{BKPUNCH} + F_{RSTRAIN}$$

or

$$F_{PUNCH} = F_{BKPUNCH} + F_{DBEAD} + F_{CTENSION}$$

Where F_{PUNCH} is the punch force and $F_{BKPUNCH}$ the backup punch force.

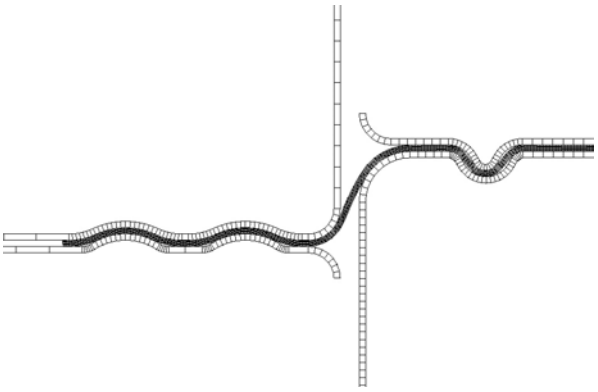

FIGURE 10. Geometry and finite element model of the stretch-flange forming operation with double draw-bead profile.

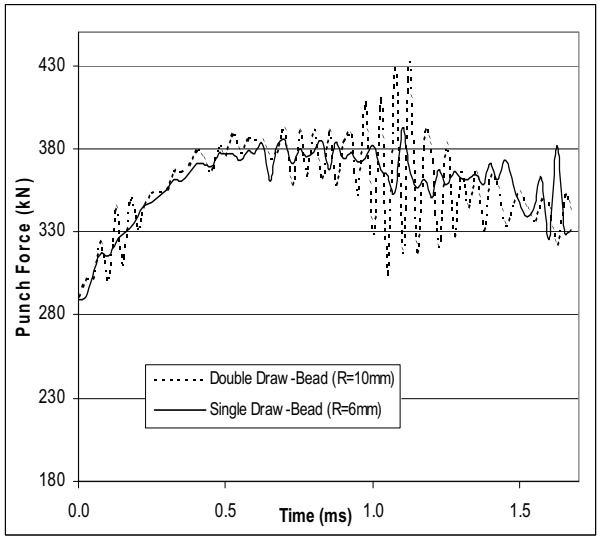

FIGURE 11. Punch force versus time.

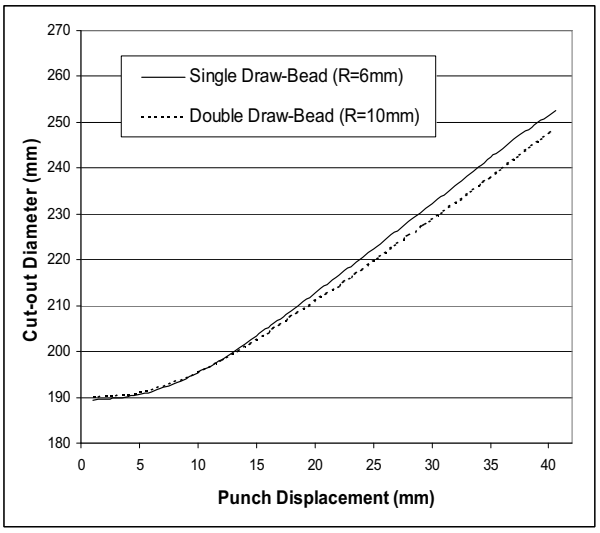

FIGURE 12. Cut-out diameter versus punch displacement

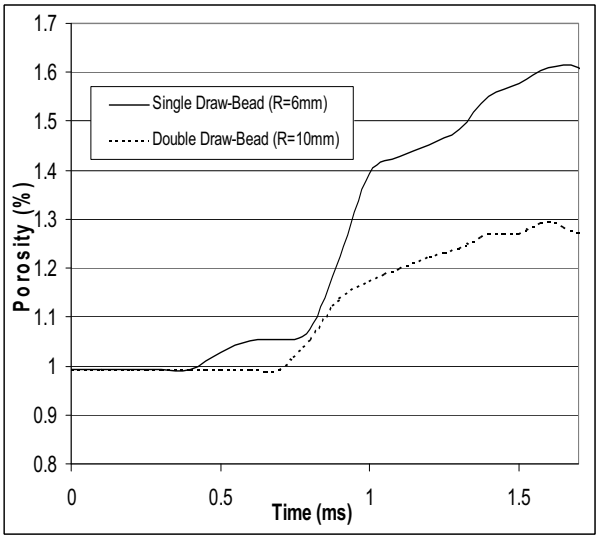

FIGURE 13. Maximum porosity versus time.

Simulations conducted on the double draw-beads with 10, 12, and 14mm radii showed that the punch force generated for the 10mm case is most comparable to that generated by the 6mm single draw-bead. This is illustrated in Figure 11 where the punch force versus time curves of the 10mm double draw-bead and 6mm single draw-bead can be seen to almost overlap. Figure 12 shows that the cut-out expansion of the blank is also similar for both draw-bead geometries. These results suggest that total restraining forces, $F_{RSTRAIN}$, produced by the 10mm double draw-bead and the 6mm single draw-bead are similar. The damage evolution of the stretch flange in terms of maximum porosity generated by the 10mm double draw-bead and 6mm single draw-bead are presented in Figure 13. Prior to 0.4μs, the maximum porosity values are

identical for both the single and double draw-bead simulations, and they originate from material damaged by the lock-beads in the clamps. After 0.4μs, damage induced by the flow of material through the draw-beads accumulates and exceeds that caused by the lock-beads, and results in a gradual increase in the maximum porosity values. In comparing the amount of porosity generated during the forming operation by the two different draw-beads in Figure 13, the amount of damage produced by the 10mm double draw-bead is found to be up to 24% less than that of the 6mm single draw-bead. These results suggest that parts formed using double draw-beads instead of single draw-beads would retain more of their original formability, which would allow for possible further development or optimization of the part.

SUMMARY

A numerical investigation to determine the level of restraining force and damage produced by single and double draw-bead geometries with different radii of curvature has been conducted. Comparison of the damage levels produced by the various draw-beads shows that the use of double draw-beads result in significantly less damage than single draw-beads with similar restraining forces. This work suggests that the substitution of single draw-beads with double draw-beads in forming operations could lead to improved formability of the part formed.

ACKNOWLEDGMENTS

This work is sponsored by Alcan International Ltd. and the Ontario Research and Development Challenge Fund.

REFERENCES

1. Cinotti, N., Shakeri, H. R., Worswick, M.J., Truttmann, S., Finn, M.J., Jain M., and Lloyd D.J., "Numerical and Experimental Investigation of Stretch-flange Forming" in *COM2000 Conference Proceedings*, 2000.

2. Worswick, M. J., and Finn, M.J., *International Journal of Plastisity* **16**, 701-720 (2000).

3. Cao, J., and Boyce, M.C., *SAE*, 930517, 145-153.

4. Michler, J. R., Weinmann, K.J., Kashani, A.R., and Majlessi, S.A., *Journal of Materials Processing Technology* **43**, 177-194 (1994).

5. Bohn, M.L., Jurthe, S.U., and Weinmann, K.J., *SAE*, 980076, 23-30.

6. Keum, Y. T., Kim, J.H., and Ghoo, B.Y., *International. Journal of Solids and Structures* **38,** 5335-5353 (2001).

7. Xu, S. G., Bohn, M.L., and Weinmann, K.J., *SAE*, 970968, 233-247.

8. Cinotti N., Shakeri H., Worswick M.J., Finn M.J., Jain M., and Lloyd D.J., "Stretch Flange Formability of Aluminum Alloy Sheet" in *Plasticity 2000 Conference Proceedings*, edited by A. Khan, 2000.

9. Orlov, O., Cinotti, N., Worswick, M.J., Lloyd D.J., and Finn, M. J., "The Role of Draw-beads in Stretch Flange Forming" in *Plasticity 2003 Conference Proceedings*, edited by A. Khan, 2003, pp. 193-195.

10. *LS-DYNA Theoretical Manual*, 1998.

11. Gurson, A. L., *J. Engng. Mater. Tech.,* **99**, 2-15 (1977).

12. Tvergaard, V., *International Journal of Fracture* **17**, 389-407 (1981).

13. Tvergaard, V., Needleman, A., *Acta Metallurgica* **32**, 157-169 (1984).